J Oceanogr (2017) 73:87–101
DOI 10.1007/s10872-016-0362-4

SPECIAL SECTION: ORIGINAL ARTICLE

Oceanographic observations after the 2011 earthquake off the Pacific coast of Tohoku

Swell-dominant surface waves observed by a moored buoy with a GPS wave sensor in Otsuchi Bay, a ria in Sanriku, Japan

Kosei Komatsu[1,2] · **Kiyoshi Tanaka**[2]

Received: 9 February 2015 / Revised: 1 March 2016 / Accepted: 7 March 2016 / Published online: 23 March 2016

Abstract Real-time monitoring of wind and surface waves in Otsuchi Bay, Iwate, Tohoku, Japan, commenced in October 2012, using a mooring buoy with an ultrasonic anemometer and a single-mode GPS wave sensor. Wind and wave data are distributed hourly in real time via the Internet along with a chart of their time series. We analyzed data monitored in the first 3 months in order to assess the variability and occurrence of wind and waves and to elucidate the main reasons for wave variation in Otsuchi Bay. The monitoring data revealed that surface waves in the bay were predominantly affected by swells propagated from the northeastern offshore region and that the wave height was significantly correlated with the component of wind velocity toward Otsuchi Bay in the northeastern offshore region that faces the bay mouth. The offshore wind field was expected to provide information useful for predicting coastal waves in a ria bay in Sanriku such as Otsuchi Bay. However, it should be emphasized that the horizontal distribution of the offshore wind field which has a significant effect on the surface waves in a ria bay depends heavily on the topographic shape of the bay.

Keywords Surface wave · Otsuchi Bay · GPS wave sensor · Swell · Ria coast

✉ Kosei Komatsu
kosei@aori.u-tokyo.ac.jp

[1] Graduate School of Frontier Sciences, University of Tokyo, 5-1-5 Kashiwanoha, Kashiwa 236-8648, Japan

[2] Atmosphere and Ocean Research Institute, University of Tokyo, 5-1-5 Kashiwanoha, Kashiwa 236-8648, Japan

1 Introduction

The 2011 earthquake off the Pacific coast of Tohoku triggered a giant tsunami, causing unprecedented damage to the Pacific coast of Tohoku, on the northeast portion of Honshu, Japan. The damaged area is composed of many ria bays, where coastal fisheries and aquacultures have traditionally been a major industry because the sea is usually not so rough and highly productive. However, the tsunami may have drastically changed the ocean ecosystem in and around the bays by causing accumulation of piles of debris on the bottom of the sea, reduction or loss of tidal flats and seaweed beds, and sedimentation of sand and mud on shore reefs. The impact of the tsunami on the ocean ecosystem must be clarified as soon as possible in order to efficiently and adequately reconstruct the coastal fisheries in the damaged area.

Otsuchi Bay, one of the ria bays in Sanriku on the Pacific coast of Tohoku, also suffered serious damage from the tsunami (Fig. 1). As is the case with the other bays, fisheries had been prosperous in Otsuchi Bay, where much effort in various fields has been made to reconstruct aquacultures of wakame seaweed, kombu kelp, scallops, oysters and sea squirts, and fishing of salmon, sea urchins, and abalone.

The state of surface waves composed of waves and swells generated by the wind is one of the most critical pieces of information for safely performing various operations in the ocean such as improvement of harbor facilities, (re)construction of aquaculture systems, removal of garbage and debris, and various fishing and aquaculture activity. Surface waves are also known to cause longshore, shoreward, and seaward (rip) currents in and adjacent to the surf zone (e.g. Mei 1989). These near-shore currents must play a significant role in transport of water mass and various organic/inorganic matter to have a physical and

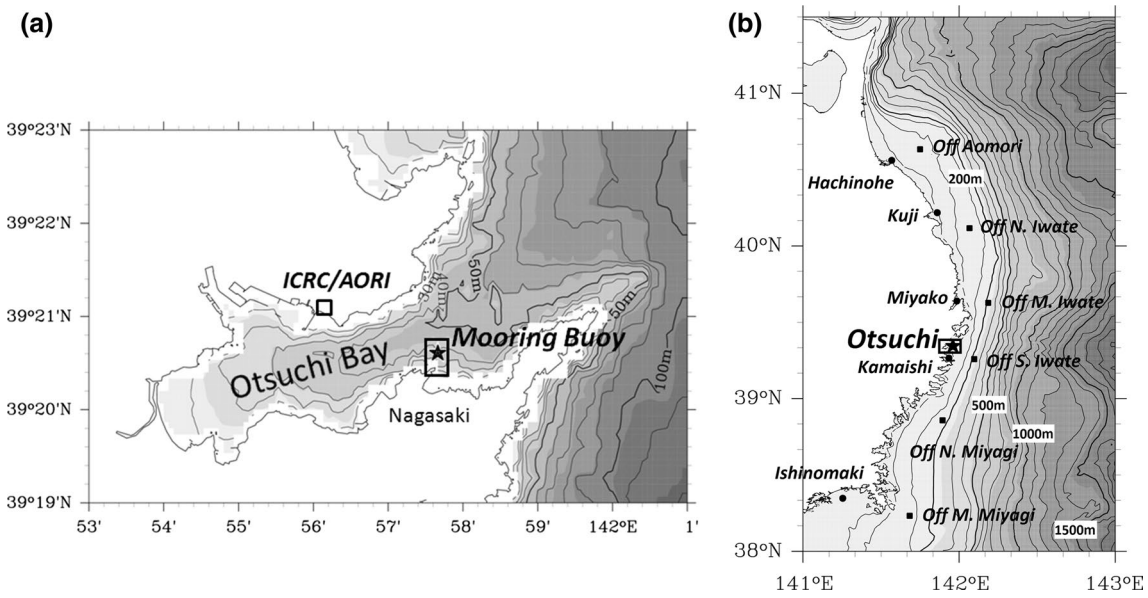

Fig. 1 **a** Mooring location of the real-time wind- and wave-monitoring buoy in Otsuchi Bay, Iwate, Japan. **b** Locations of wave monitoring stations in the Pacific coast of Tohoku, where Otsuchi Bay is enclosed by a *rectangle*. Stations, except for our buoy (*closed stars*), belong to the wave information network NOWPHAS of the Ministry of Land, Infrastructure, Transport, and Tourism, Japan. RTK-GPS wave recorders are used in the offshore stations (*closed square*) and ultrasonic recorders are bottom-mounted in the inshore ones (*closed circles*)

biogeochemical impact on the coastal ecosystem. Moreover, the breaking of surface waves generates successive turbulence (e.g. Agrawal et al. 1992; Craig and Banner 1994; Melville 1996; Feddersen and Trowbridge 2005), which also influences the coastal ecosystem by mixing of seawater, diffusion of various animate/inanimate objects, gas exchange at the sea surface, and the maintenance of ecosystem balance. As an ecologically interesting example, wave-induced turbulence effectively adjusts the balance between seaweed and herbivores such as sea urchins and abalone by restraining their grazing (Kawamata 2001).

However, there has never been any observation of surface waves in Otsuchi Bay, although profilings of water properties and currents have been monitored continuously and several biogeochemical observations have been conducted periodically in the bay (e.g. Otobe et al. 2009). Therefore, the effects of surface waves previously mentioned have been unknown in the bay.

On the Pacific coast of Tohoku, surface waves are monitored continuously by the Nationwide Ocean Wave information network for Ports and HArbourS (NOWPHAS), managed mainly by the Bureau of Ports and Harbors, Ministry of Land, Infrastructure, Transport, and Tourism, Japan (Fig. 1b). Although two monitoring sites of NOWPHAS are located within 50 km of both the north and south sides of Otsuchi Bay, the state and characteristics of surface waves are empirically known to be different even in two adjacent bays. The wave state in the bay, therefore, cannot be predicted correctly by simply applying data observed in the adjacent bays.

On the other hand, a recent numerical simulation has achieved such high precision that it is now the most powerful tool for estimating the state of surface waves (e.g. The WAMDI Group 1988; Tolman 2002). While operational wave models have successfully reproduced wave fields in deep water, they need various modifications and sometimes ad hoc adjustments on the basis of in situ data for application to finite-depth and shallow-water waves in coastal regions, depending on topography (e.g. Booij et al. 1999; Ris et al. 1999; Zijlema et al. 2011; Buckley et al. 2014). No numerical model has ever been applied to Otsuchi Bay, where at present there is no way to correctly estimate the state and characteristics of surface waves.

Previous studies of surface waves on the Pacific coast of Tohoku have found a significant correlation in significant wave height and period between the coastal and offshore waves from statistical analyses of NOWPHAS data (Kawaguchi et al. 2011; Kawai et al. 2012). The occurrence probability of swells was found to be higher in the Pacific coast than in the coast of the Japan Sea from coastal wave data monitored by the Japan Meteorological Agency (Sugimoto and Chikasawa 2008). These results suggest that swells propagated from the offshore region have a significant impact on the energy and its variation of surface waves observed on the Pacific coast, but none of the previous studies have demonstrated the impact of swells quantitatively,

as far as we know. Coastal surface waves are mixtures of swells propagated from the offshore region and wind waves generated by local wind, and are more or less under the shallow water effects. Two-dimensional spectral analysis of waves and observation of wind at the same point as surface waves are the minimal requirements to clarify the impact of swells quantitatively.

We, therefore, began real-time monitoring of surface waves and wind in Otsuchi Bay on October 3, 2012 using a mooring buoy with an ultrasonic anemometer and a single-mode GPS wave sensor. The monitoring buoy is the first to observe wind and directional (2D) spectra of surface waves continuously and at the same place in the Pacific coast of Tohoku. The monitoring objectives are (1) to distribute data of wind and waves to help fisheries and various works in and around the bay, (2) to clarify the actual state and characteristics of wind and waves, especially to evaluate quantitatively impacts of swell on waves in the bay, (3) to investigate impacts of surface waves on the bay ecosystem as mentioned above, and (4) to provide in situ data to validate the accuracy of numerical models.

In this study, we aim to clarify the variability and occurrence of wind and waves in Otsuchi Bay, in particular to evaluate quantitatively contributions of swells from the offshore region and wind waves to the total wave energy in the bay. For this purpose, we analyzed wind data and directional wave spectra observed by the mooring buoy in the first 3 months of monitoring; throughout the period, we, fortunately, obtained data completely without any serious troubles. The first 3 months corresponds to autumn in 2012, the study does not cover the other seasons. However, Sugimoto and Chikasawa (2008) indicate that influences of swell on coastal waves are observed throughout the year using long-term observational data. Conclusions of the study probably do not need drastic modifications as discussed later, even though the extent of swell's influence changes seasonally.

2 Real-time monitoring of wind and waves in Otsuchi Bay

2.1 Structure of mooring buoy

Otsuchi Bay is one of the ria bays located in Sanriku, in the northeast of Japan. Its mouth opens to the northeast and toward the Pacific with a width of 3 km (Fig. 1). A real-time monitoring buoy with an ultrasonic anemometer and a single-mode GPS wave sensor was moored using polypropylene ropes with floats and sandbag anchors to two points on the bay's bottom (40 m depth) at a position of 39°20.65′N, 141°57.62′E, which is 300 m north of the southern coast of Otsuchi Bay (Figs. 1, 2a). The mooring system was configured not to overlap the adjacent aquaculture areas. The distance between the two anchors is 90 m, which is equal to the total length of ropes connected at the sea surface, as shown in Fig. 2b. The surface ropes, therefore, are ordinarily so slack that the buoy remains free from constraint.

The buoy is a custom product manufactured by Zeni Lite Buoy Co., Ltd and is designed on the basis of commercially available buoys to respond appropriately to wind waves. It is composed of an ultrasonic anemometer, a single-mode GPS wave sensor, a transmitter–receiver, an internal recording device, a statistical processing unit, solar panels, batteries and a disc-like float made of expanded polystyrene (Fig. 2c). Compared with conventional observation stations, it is considerably more compact, with a total height of 2.1 m and with a diameter of 1.1 m. It is also relatively light by total weight in air of 90 kg (total buoyancy of 120 kg), so that it can be easily handled by a small boat for maintenance. It runs entirely on electric power supplied by the solar panels and needs no supply from land. Maintenance of the buoy is supported by the International Coastal Research Center of the Atmosphere and Ocean Research Institute (ICRC/AORI) at the University of Tokyo.

It should be emphasized that the monitoring system enabled us to estimate quantitatively contributions of swell and wind waves to the total wave energy in a ria bay by using directional (2D) wave spectra and wind data, although it is a low-cost system different from existing facilities such as observation towers and weather buoys.

2.2 Monitoring of wind

Horizontal wind velocity is measured by an ultrasonic anemometer with a two-axis wind sensor (Model 32500, R. M. Young Company) installed at a height of 1.5 m on the float. Measurements are conducted hourly for 10 min just before the hour, at 0.5 s intervals. Three dimensional fluctuation of the buoy causes errors of the wind direction and velocity. The direction error is corrected by an adjunctive electronic compass that provides accurate magnetic-heading indications. The velocity error cannot be corrected in real time but can be decreased by subtracting velocity of the buoy estimated from its displacement measured at 0.4 s intervals. Continuous wind data are recorded on a secure digital (SD) card attached to the inside of the buoy, and statistical calculations of averaged speed and direction, and maximum instantaneous speed and its direction over each 10-min period are transmitted via an Iridium satellite to the data server in real time. The study uses not the instantaneous wind data but the corrected ones averaged over 10-min. The influence of the contamination of the buoy fluctuation on the averaged wind speed was less than 1 ms^{-1}.

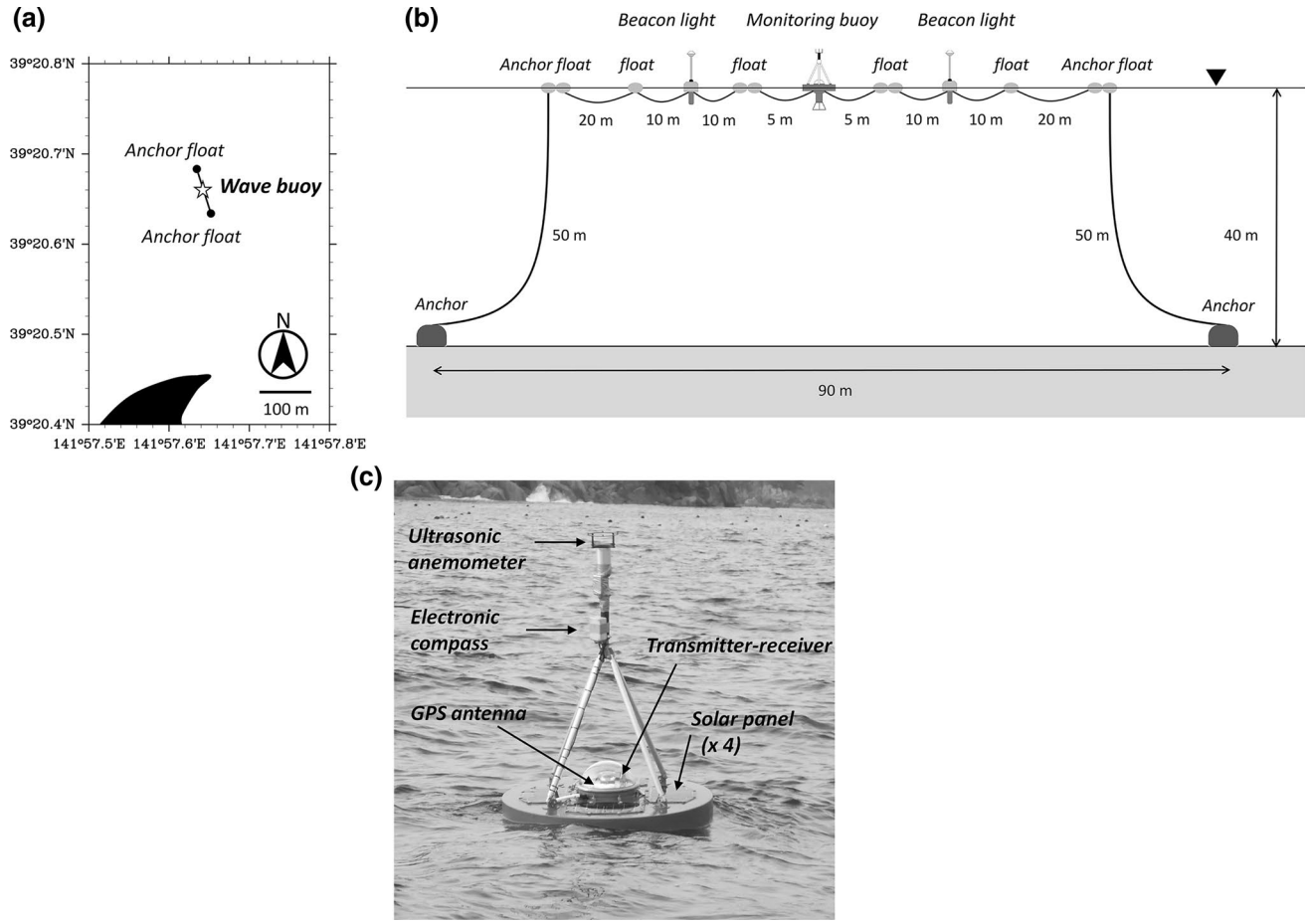

Fig. 2 **a** Plan view of the mooring point in Otsuchi Bay, **b** schematic sectional view of the mooring system, **c** real-time wind- and wave-monitoring buoy

2.3 Monitoring of surface waves

Wave height, wave period, and wave direction are measured from the 3D displacement of the buoy hourly in 0.4-s interval for 20 min just after the hour, using a single-mode GPS sensor attached to the top face of the float. Unlike real-time kinematic (RTK) or differential GPS schemes, the single-mode sensor uses only one GPS receiver and requires neither reference stations nor other facilities, so that it can be set up at considerably lower cost and be handled with comparative ease.

On the other hand, it cannot be positioned as accurately as the other GPS sensors. Its accuracy is less than 1/10 that of the other sensors because of errors inherent in the GPS system, caused mainly by ephemeral shifts and clock errors of satellites, ionospheric and tropospheric effects, and multipath effects (Hofmann-Wellenhof et al. 2007). Errors in the GPS system, however, are characterized by time scales longer than 100 s, while the wave periods of wind waves are not longer than 20–30 s in almost all cases. Therefore, our buoy adopts a type of high-pass filtering algorithm developed by Harigae et al. (2004), who were able to measure wind waves with an operationally sufficient accuracy in comparison with an ultrasonic wave sensor and an accelerometer by filtering out errors reasonably and efficiently (Harigae et al. 2004). Laboratory tests show that the algorithm achieved an accuracy of several cm in wave height, less than 1 s in wave period and several degrees in wave direction (Harigae et al. 2004). Comparison with accelerometer wave sensors in field experiments indicates that GPS-based wave sensors are sufficiently accurate to replace existing wave sensors (Harigae et al. 2004). Recently, wave measurements using a similar type of buoy equipped with a GPS-based wave sensor were conducted successfully in several regions (e.g. Waseda et al. 2014).

Corrected 3D displacements of the buoy and wind velocities are recorded hourly on the SD card, and wave statistics over the 20-min periods are calculated simultaneously using the zero-up-crossing method. Wave parameters including significant wave height $H_{1/3}$, maximum wave height H_{max}, and 1/10 maximum wave height $H_{1/10}$, along with their corresponding wave periods ($T_{1/3}$, T_{max}, and

$T_{1/10}$) and directions ($\theta_{1/3}$, θ_{max}, and $\theta_{1/10}$) are transmitted to the data server in real time along with the number of waves detected in the 20-min intervals. $H_{1/3}$ and $H_{1/10}$ are defined traditionally as the mean wave height (trough to crest) of the highest third and tenth of the waves, respectively.

2.4 Real-time distribution of monitoring data

Statistics are calculated for resolutions of 0.01 m, 0.1 s, 1°, 0.1 ms^{-1} and 1° for wave height, wave period, wave direction, wind speed, and wind direction, respectively. Mean wind velocity and direction, along with the significant wave height and its corresponding wave period and direction, are distributed in real time on the web, along with charts of their time series (http://lmr.aori.u-tokyo.ac.jp/feog/kosei/ootuchi/nagasaki.html), which can be viewed through cellular phones and used by local fishermen to plan a fishing schedule.

3 Results

3.1 Characteristics of wind and waves in Otsuchi Bay

3.1.1 Temporal variation

A time series of wind and waves for 3 months after the monitoring commenced in Otsuchi Bay is shown in Fig. 3. Significant wave heights $H_{1/3}$ are usually lower than 1 m but intermittently beyond 1 m (Fig. 3a). Significant wave

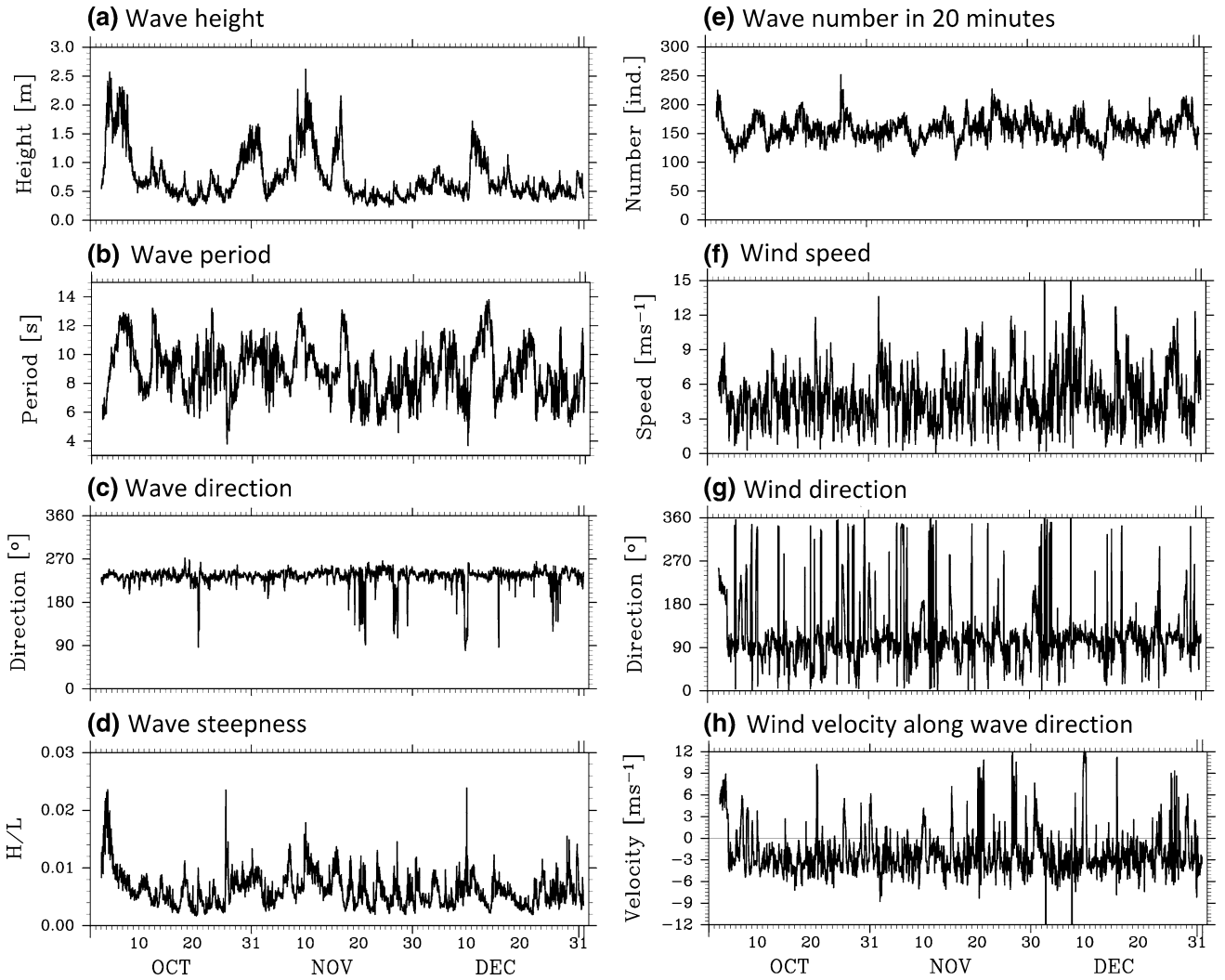

Fig. 3 Time series of hourly statistics for surface waves and wind calculated by the real-time monitoring buoy in Otsuchi Bay. The *line* denotes the significant wave height (**a**), its wave period (**b**), wave direction (**c**), wave steepness (**d**), and number of individual waves in 20-min periods (**e**). Wind speed (**f**) and direction (**g**) are represented by 10-min averages, and wind velocities along the direction of the significant wave are shown (**h**). "Wave direction" denotes the propagation direction; "wind direction" denotes the direction toward which wind was blowing

periods $T_{1/3}$ appear to be longer in higher wave cases as a whole; however, the relationship between $H_{1/3}$ and $T_{1/3}$ is not so simple (Fig. 3b). The significant wave direction $\theta_{1/3}$, which is defined as the direction in which the waves are propagating, was approximately 210°–250° with small fluctuations (Fig. 3c), indicating that waves propagating southwestward or toward the inner part of the bay are dominant in the bay. Wave steepness, defined as $H_{1/3}/L_{1/3}$, changes from 0.002 to 0.02 with some exceptions (Fig. 3d); however, its magnitude is small (usually <0.01) in comparison with waves observed in offshore regions as reported by Sugimoto and Chikasawa (2008), where significant wave length $L_{1/3}$ was calculated using the linear dispersion relation for finite-depth water waves. The number of individual waves counted by the zero-up-cross method in 20 min was between 100 and 200 (Fig. 3e).

Mean wind speed fluctuated sharply and seldom exceeded 10 ms^{-1} (Fig. 3f). Mean wind direction, defined as the direction toward which wind was blowing, was usually about 70°–130° (Fig. 3g), indicating that waves blowing through east–southeastward or offshore are dominant in the bay. The component of mean wind velocity along the significant wave direction $\theta_{1/3}$ was negative in most cases, indicating that wind direction and wave direction were opposite.

The occurrence probability of significant wave height, period, steepness, and direction, along with mean wind speed and direction, are shown in Fig. 4 with the average (Avg) and the standard deviation (σ), where Avg $\pm$ σ corresponds to 0.75 $\pm$ 0.43 m, 8.8 $\pm$ 1.8 s, 0.0063 $\pm$ 0.0030, 230° $\pm$ 20°, 5.0 $\pm$ 3.7 ms^{-1}, and 116° $\pm$ 67°, respectively.

3.1.2 Exceedance probability

The exceedance probability, defined as the probability that a given level of a wave event will be exceeded, of significant wave height, period, and steepness in Otsuchi Bay was compared with those observed at other sites in and around the Sanriku Coast by the NOWPHAS. Waves analyzed here are observed using an ultrasonic recorder mounted on the bottom at coastal sites Hachinohe, Kuji, Miyako, Kamaishi, and Ishinomaki. A RTK-GPS wave recorder was used at sites offshore from Aomori, North Iwate, Mid Iwate, South Iwate, North Miyagi, and Mid Miyagi (Fig. 1b).

Exceedance probability for significant wave height was reported by Sugimoto and Chikasawa (2008) to be higher in waves observed in offshore regions, especially where $H_{1/3}$ is higher than 1 m (Fig. 5a). This indicates that waves are attenuated in the shallow water region by effects such as deformation and breaking as they propagate from offshore to coastal regions (Ardhuin et al. 2003). It should be emphasized that the probability of significant wave height is lowest on the whole in Otsuchi Bay. In a more detailed comparison, Miyako and Ishinomaki stations yield lower probabilities to the same extent as Otsuchi Bay for $H_{1/3}$ over 2 m. Comparatively, a narrow bay mouth is common to both Ostuchi and Miyako bays, as shown later in Fig. 12; therefore, offshore waves propagating toward the bays may be shaded more strongly by the capes stuck out from the bay mouth.

On the other hand, for the significant wave period shorter than 13 s, the exceedance probability is the highest in Kamaishi Bay and the second highest in Otsuchi Bay (Fig. 5b). Differently from $H_{1/3}$, the exceedance probability of $T_{1/3}$ cannot be divided clearly into coastal and offshore waves (Fig. 5b). The high exceedance probability in Kamaishi and Otsuchi Bays may be attributed to their long distance from the source region of swells. If the main source of swells which dominantly impact on coastal waves in both bays is located in the northeastern offshore region as discussed later, the long distance from the source region can cause a longer wave period by downshift of the spectral peak frequency due to the nonlinear quadruplet wave–wave interaction (e.g. Komatsu and Masuda 1996).

These factors lead to lower wave steepness in coastal waves. Especially in Otsuchi Bay, wave steepness is extremely small (Fig. 5c), reflecting its lower and longer waves. The exceedance probability of the wave steepness is comparatively low also in Miyako and Kamaishi bays both of which are close to Otsuchi Bay (Fig. 1b); however, there is no station that presents both lower probability for high $H_{1/3}$ and higher probability for long $T_{1/3}$ in comparison with our station in Otsuchi Bay. Not only the observational studies but also numerical ones with high precision are necessary to clarify the reason why the wave steepness is the smallest in Otsuchi Bay.

3.2 Relationship to offshore waves

In Otsuchi Bay, dominant waves propagated in a direction about 110° different from the mean wind, as discussed above. The direction from which the dominant waves propagate is consistent with the direction in which the mouth of Otsuchi Bay opens to the ocean. This consistency suggests that the dominant waves are not wind waves developed by local wind in the bay but swells propagated from the offshore region. There was no significant correlation between the significant wave height $H_{1/3}$ and the component of wind velocity along the significant wave direction $\theta_{1/3}$ in the bay (Fig. 6). Therefore, $H_{1/3}$ in Otsuchi Bay was compared with one observed in the same period at the NOWPHAS site "Off Mid Iwate" (hereinafter, M. Iwate), which is located offshore from the northeastern side of the bay (Fig. 1b).

A scatter diagram of significant wave heights recorded in Otsuchi Bay and at the offshore M. Iwate station is

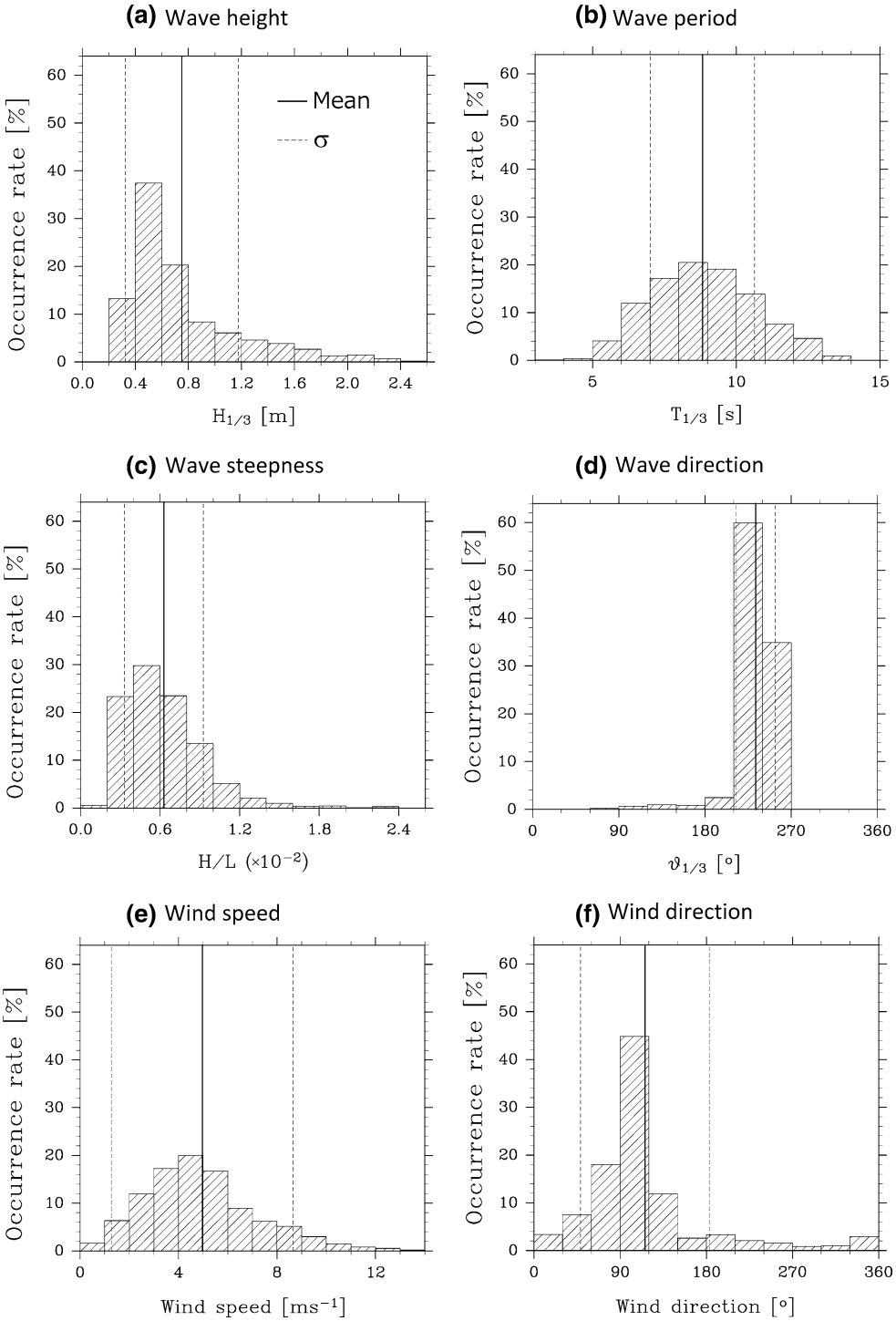

Fig. 4 Occurrence probability of $H_{1/3}$ (**a**), $T_{1/3}$ (**b**), wave steepness $H_{1/3}/L_{1/3}$ (**c**), $\theta_{1/3}$ (**d**), mean wind speed (**e**), and mean wind direction (**f**) in Otsuchi Bay from October 3 to December 31, 2012. The *thick solid vertical line* denotes the average, and the *dashed line* denotes the standard deviation

shown in Fig. 7a. As seen before, the offshore waves were higher than the coastal waves in the bay. Lag correlation between the two wave heights yielded a maximum coefficient of 0.65 at the time lag of −3 h (Fig. 7b), suggesting that offshore waves have a significant effect on the variability of coastal waves in the bay. Extraction of waves propagating southwestward (210°–240°) at the M. Iwate station resulted in a stronger correlation between the wave heights (Fig. 7a), whose maximum coefficient was 0.83 (Fig. 7b), as is the case in other stations in the Pacific coast of Tohoku (Kawaguchi et al. 2011; Kawai et al. 2012). Least squares analysis generated a regression line in which $H_{1/3\text{ at M. Iwate}} = 1.9 \times H_{1/3\text{ at Otsuchi}}$ ($R^2 = 0.76$, Fig. 7a), meaning that, in this case, wave height in the bay can be estimated at about half of the height at the M. Iwate site.

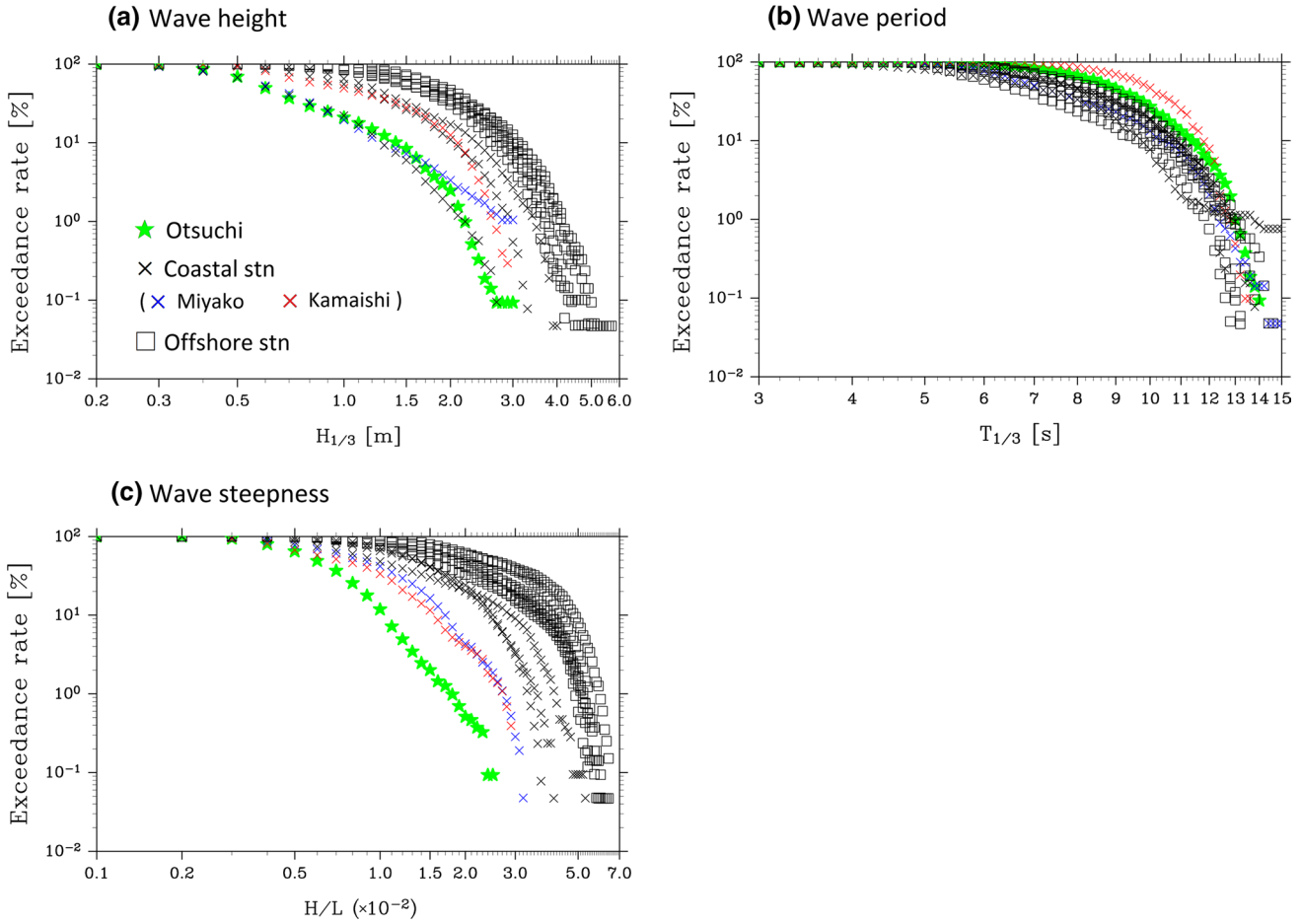

Fig. 5 Exceedance probability of $H_{1/3}$ (**a**), $T_{1/3}$ (**b**), and wave steepness $H_{1/3}/L_{1/3}$ (**c**) calculated in the Tohoku area from 3 October to 31 December 2012. Probabilities calculated in Otsuchi Bay and at the NOWPHAS coastal and offshore stations are denoted by *stars*, *crosses*, and *squares*, respectively. *Blue* and *red crosses* denote probabilities observed inside Miyako Bay and Kamaishi Bay, respectively, which are adjacent to Otsuchi Bay

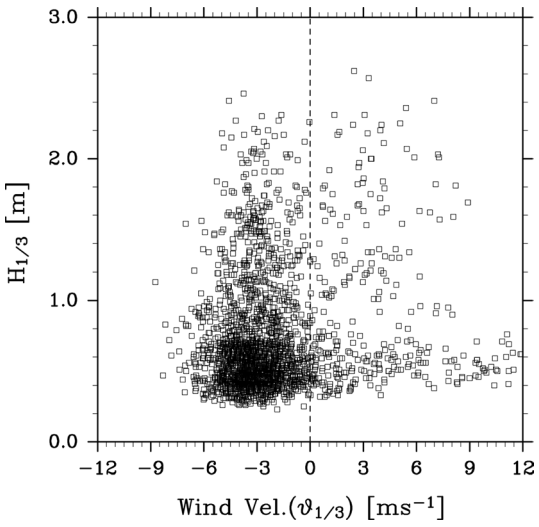

Fig. 6 Relationship between the wind velocity along the wave direction and the significant wave height recorded in Otsuchi Bay

On the other hand, correlation with waves observed at the NOWPHAS site "Off South Iwate" (hereinafter, S. Iwate), which is the closest offshore station of the NOWPHAS, is weak in comparison with the correlation with waves at the M. Iwate station (Fig. 7c). The correlation is not so strong even when extracting waves propagating northwestward (290°–320°), as shown in Fig. 7c. The results suggest that waves in the bay apparently change under the strong influence of southwestward-propagating swells.

Figure 7b indicates the maximum correlation coefficient with no significant time lag. Waves are supposed to take 1.4 h to propagate from M. Iwate to Otsuchi Bay if the group velocity of deep water is applied to the averaged waves whose period is 9 s (Fig. 4b); however, the relationship between the waves in the bay and offshore waves does not seem so simple.

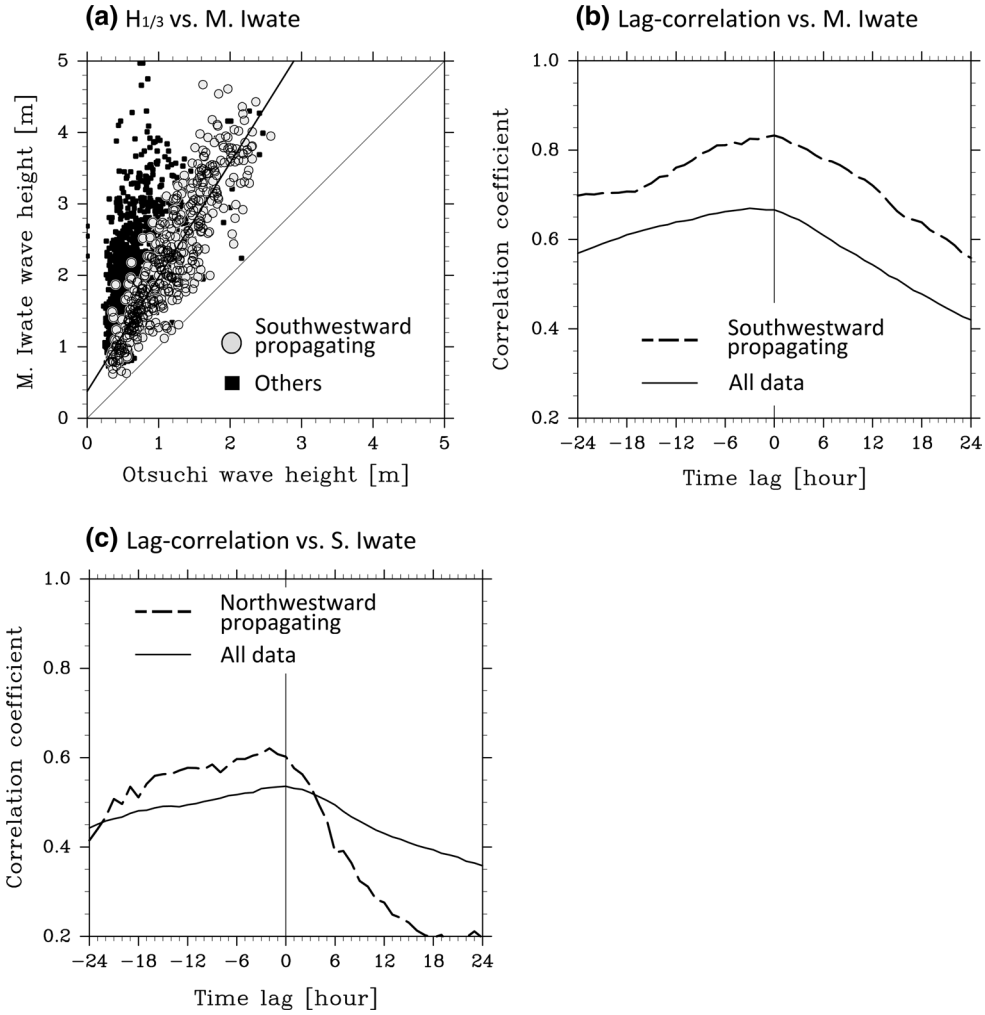

Fig. 7 **a** Relationship between significant wave heights recorded in Otsuchi Bay and those at the offshore M. Iwate station of NOWPHAS. *Gray circles* denote waves propagating southwestward (210°–240°) at the M. Iwate station. The *thick black line* indicates the regression line. **b** Lag correlation between significant wave heights in Otsuchi Bay and those at the M. Iwate station. The *dashed line* indicates the correlation for waves propagating southwestward at the M. Iwate station. **c** Same as in **b** but for the S. Iwate station. The *dashed line* indicates the correlation for waves propagating northwestward (290°–320°) at the S. Iwate station

3.3 Contribution of swells

3.3.1 Directional wave spectrum

The above results suggest strong influences of swells on surface waves in Otsuchi Bay; however, they cannot be evaluated quantitatively by the statistics such as significant wave height and period. Quantitative estimation of the contribution of swells to the total wave energy requires the directional (2D) wave spectrum of the energy density in the f–θ domain, where f denotes the wave frequency (s^{-1}), and θ the wave direction (°). The wave spectra observed in Otsuchi Bay can be calculated hourly from continuous records of the 3D displacement of the buoy sampled over 20 min with 0.4-s intervals. Sea surface elevation η and horizontal velocities of water particles (u, v) were inferred from the buoy displacements, then directional wave spectra $F(f, \theta)$ were derived calculating cross spectra from the time series of η, u, and v by applying the scheme presented by Isobe et al. (1984a, b).

First of all, example analysis was conducted to confirm the capability of separating swells from wind waves by use of the directional wave spectra observed in Otsuchi Bay. Directional wave spectra in typical cases of both high and low significant wave heights are shown in Fig. 8a, b. Both spectra indicate highly concentrated distributions in the wave frequency–direction coordinate system, with spectral peaks located at 0.07–0.08 s^{-1} in the frequency domain and at 230°–240° in the directional one. More specifically, the high-wave example shows an unimodal distribution (Fig. 8a); on the other hand, the low-wave example shows another local maximum located at the high frequency side (~0.5 s^{-1}) and around 90° (Fig. 8b). In the latter case, the bimodal distribution can be identified more clearly from the frequency (1D) spectra $F_1(f)$ which is calculated by integrating $F(f, \theta)$ in the θ domain as shown in Fig. 8c:

$$F_1(f) = \int_0^{360} F(f, \theta) \mathrm{d}\theta \quad (1)$$

The latter case indicates that the main spectral peak is lower and down-shifted, and a more conspicuous bump is

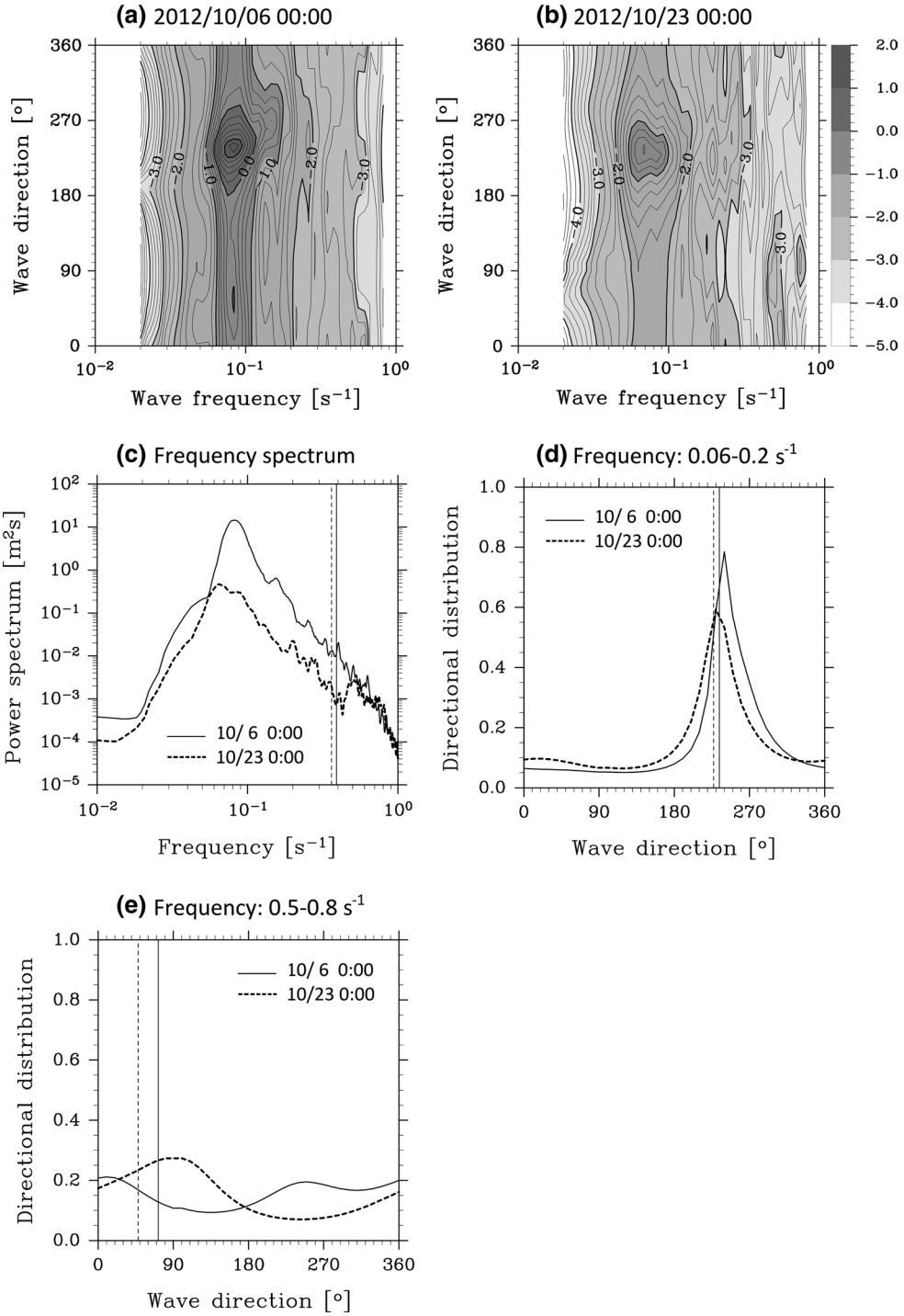

Fig. 8 **a** Directional wave spectrum calculated from the record in Otsuchi Bay in October 6, 2012, 0:00–0:20, when comparatively high $H_{1/3}$ was observed. *Contour lines* are rendered using a logarithmic scale. **b** Same as in **a** but for the directional wave spectrum in October 23, 2012, 0:00–0:20, when comparatively low $H_{1/3}$ was observed. **c** Frequency wave spectra $F_1(f)$ observed in the above periods. The *solid* (*dashed*) *vertical line* denotes the separation frequency for the spectrum in October 6 (23). **d** Directional distribution of the wave spectrum averaged in the frequency range from 0.06 to 0.2 (s^{-1}), where swells are predominant in most cases. The *solid* (*dashed*) *vertical line* denotes the significant wave direction in October 6 (23). **e** Same as in **d** but for one averaged in the frequency range from 0.5 to 0.8 (s^{-1}), where wind waves are predominant in most cases. The *solid* (*dashed*) *vertical line* denotes the wind direction in October 6 (23)

distributed on the high frequency side (Fig. 8c). Time series of the frequency spectrum indicates that spectral peaks are located in the frequency band of 0.07–0.2 s^{-1} and their magnitude synchronizes with the significant wave height (Figs. 3a, 9a). The result indirectly suggests that long-period swells are predominant in surface waves in Otsuchi Bay, because the significant wave height corresponds approximately to $4\sqrt{E_{\text{total}}}$ (Forristall 1978), where E_{total} is the total wave energy calculated by integrating the directional spectrum in the f–θ domain:

$$E_{\text{total}} = \int_{f_{\min}}^{f_{\max}} \int_{0}^{360} F(f,\theta)\mathrm{d}\theta\, df, \tag{2}$$

where $f_{\max}$ (= 1.0 s^{-1}) and $f_{\min}$ (= 0.01 s^{-1}) are the maximum and minimum of the frequency domain, respectively.

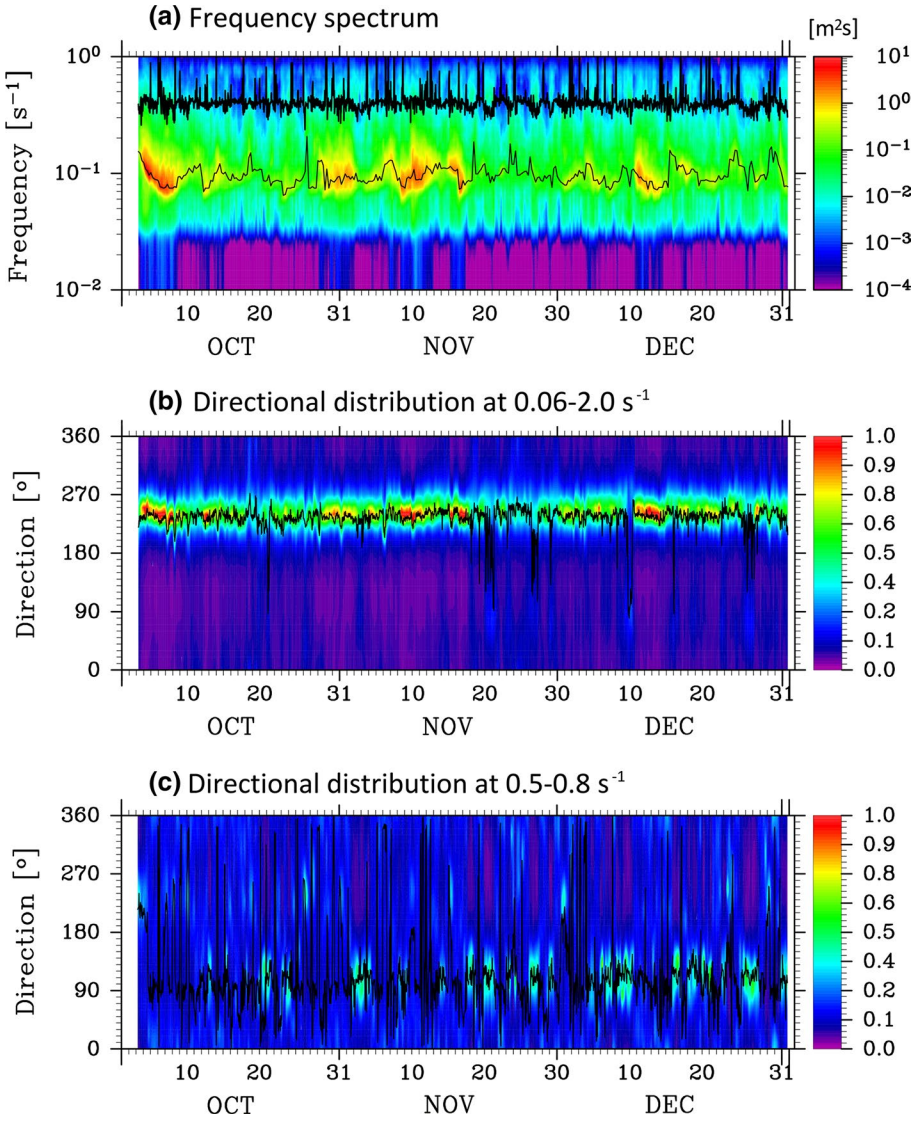

Fig. 9 **a** Time series of the frequency wave spectrum in Otsuchi Bay. *Thin* and *thick black lines* denote the spectral peak and separation frequencies, respectively. **b** Time series of the directional distribution of the wave spectrum averaged in the frequency band of 0.06–0.2 (s^{-1}). The *black line* denotes the time series of the significant wave direction. **c** Same as in Fig. 8d but for one averaged in the frequency band of 0.5 to 0.8 (s^{-1}). The *black line* denotes the time series of the wind direction

Moreover, the contribution of swells and wind waves can be recognized also in the directional distribution of the wave spectra $D(f, \theta)$, which is defined as

$$D(f,\theta) = F(f,\theta)/F_1(f) \tag{3}$$

For example, directional distributions averaged in the frequency range of 0.06–0.2 and 0.5–0.8 s^{-1} are shown in Fig. 8d, e, respectively. The former directional distributions are concentrated in both cases, and their peaks are located in the direction almost consistent with the significant wave direction (Fig. 8d). A time series of the directional distribution indicates that the direction of concentrated peaks almost agrees with the significant wave direction within the direction band of 220°–260° (Fig. 9b) throughout the period, and that the magnitude of the concentrated peak synchronizes with that of the peak of $F_1(f)$ in Fig. 9a. The results suggest that directionally concentrated swells are related to higher waves in Otsuchi Bay.

On the other hand, the latter directional distributions at higher frequencies are broader and the direction of their maxima is not so close to the wind direction (Fig. 8e). However, a time series of the directional distribution indicates that the direction of the concentrated peak larger than 0.4 seems consistent with the wind direction (Fig. 9c). The results suggest the contribution of locally generated wind waves to the high frequency components of wave spectra.

3.3.2 Separation of swell and wind waves

The above results support the validity of separating swells from wind waves by use of the directional spectra observed in Otsuchi Bay. The study, therefore, applied the algorithm of Portilla et al. (2009) to automatically identify swells and wind waves. The algorithm acquires robustness by using both the directional spectrum and the wind data, where U_{10}, the neutral wind speed at 10 m above mean sea level, was

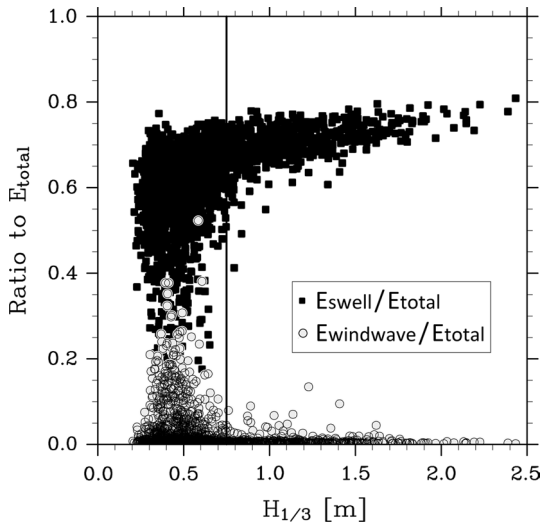

Fig. 10 Relationships of E_{swell}/E_{total} and $E_{windwave}/E_{total}$ to $H_{1/3}$ in Otsuchi Bay. 6-h averages are plotted

estimated from the horizontal wind speed measured by the ultrasonic anemometer mounted on the mooring buoy on the assumption of the logarithmic vertical-profile of wind speed, using the typical drag coefficient presented by Large and Pond (1981). Examples of the separation frequency f_s estimated from the algorithm are shown in Fig. 8c, where f_s seems to separate swells from wind waves appropriately. A time series reveals that f_s is fluctuating and located in the frequency domain higher than 0.3 s^{-1} (Fig. 9a).

Wave energies of swells and wind waves can be calculated automatically by integrating the directional wave spectrum over the f–θ domain identified by the algorithm of Portilla et al. (2009). Contributions of swells and wind waves to the total wave energy are expressed by E_{swell}/E_{total} and $E_{windwave}/E_{total}$, respectively, where E_{swell} is the swell energy and $E_{windwave}$ is the energy of wind waves. Relationships of the contributions to $H_{1/3}$ shown in Fig. 10 indicate that swells propagated from the offshore region contribute 60–80 % of the total wave energy (corresponding to about 80–90 % of $H_{1/3}$) observed in Otsuchi Bay in the higher wave case (>averaged $H_{1/3}$). On the other hand, contribution of wind waves generated in the bay was less than 15 %, except for the lower wave case ($H_{1/3}$ <averaged $H_{1/3}$).

These observations support the conclusion that the variability of surface waves in Otsuchi Bay are strongly dependent on that of swells propagated from the northeastern offshore region into the bay.

4 Discussion

Surface waves observed in Otsuchi Bay were found to vary in response to swells propagated southwestward into the bay from the offshore region. The swells were originally generated and developed by offshore local wind, so that monitoring of wind velocity over the offshore region is expected to enable us to predict the variability of waves in the bay with a certain degree of accuracy without resorting to complicated numerical simulations, if a clear relationship is found between the waves in the bay and offshore wind.

Time-lag correlation coefficients were calculated between significant wave heights in Otsuchi Bay and wind velocity fields at 10-m heights, as objectively analyzed by the mesoscale model of the Japan Meteorological Agency (MSM-GPV) in the period from October through December 2012. The wind velocity incorporated the component in the direction of Otsuchi Bay from each grid point of the wind field in the calculation with a temporal resolution of 1 h and horizontal resolution of 0.05° × 0.0625°. The horizontal distribution of the maximum correlation coefficient is shown in Fig. 11a. A relatively high coefficient (>0.4, $p < 0.05$) is recorded in the northeastern region from Otsuchi Bay, which almost overlaps with the region between the two extended lines from the northern and southern coast lines of the bay mouth. In the high-coefficient region, the time lag was between −30 and −10 h, and shifts more negatively when departing farther toward the offshore region from the bay (not shown in the figure). The time lag might correspond to the elapsed time required for dominant waves generated originally by the local wind to arrive from the offshore point in the bay.

To examine the relationship between the wind speed and the correlation coefficient, the occurrence rate of hourly wind velocities toward Otsuchi Bay was calculated for velocities beyond 5 ms^{-1} at each grid point (Fig. 11b). The occurrence rate was higher than 15 % in the northeastern region, which includes the region where the maximum correlation coefficient was higher than 0.5 (Fig. 11a). This high frequency indicates that waves generated by local southwestward wind in the northeastern region propagate directly as swells into the bay to affect predominantly the variation of waves in the bay. On the other hand, the occurrence rate of wind velocity over 5 ms^{-1} was also higher than 15 % in the southeastern region (Fig. 11b), where the maximum correlation coefficient was lower rather than higher in comparison with the neighboring region (Fig. 11a). This circumstance may exist because the southern headland of the bay mouth prevents waves originating from the southeastern region from propagating directly into the bay, so that waves generated by local southeasterly wind cannot directly impact the characteristics of waves in the bay.

Surface waves begin to be affected by the ocean bottom when they propagate into shallow-water regions adjacent to the coast. We must consider several processes such as

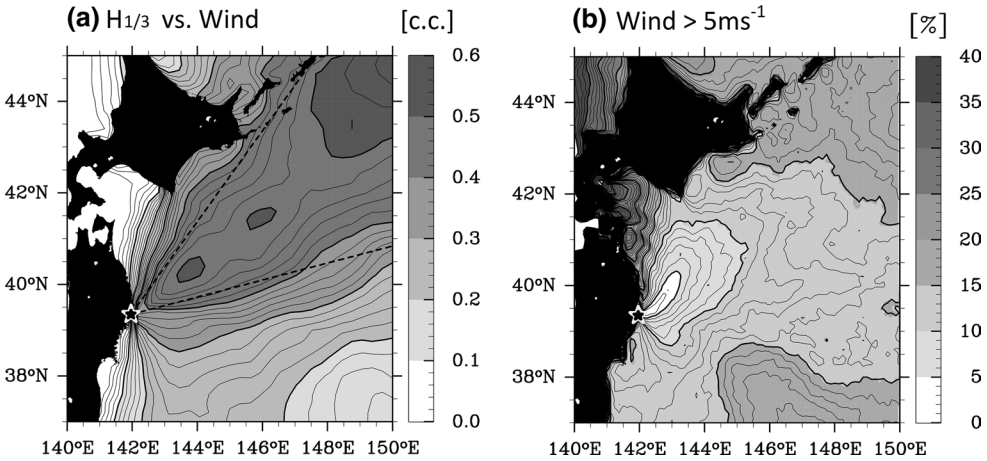

Fig. 11 **a** Horizontal distribution of maximum correlation coefficient between significant wave height in Otsuchi Bay and wind velocity toward Otsuchi Bay from each grid point. The *star* indicates the location of the station in Otsuchi Bay and the *dashed line* indicates the direction extended from the bay mouth. **b** Occurrence rate of wind velocity toward Otsuchi Bay over 5 ms^{-1}

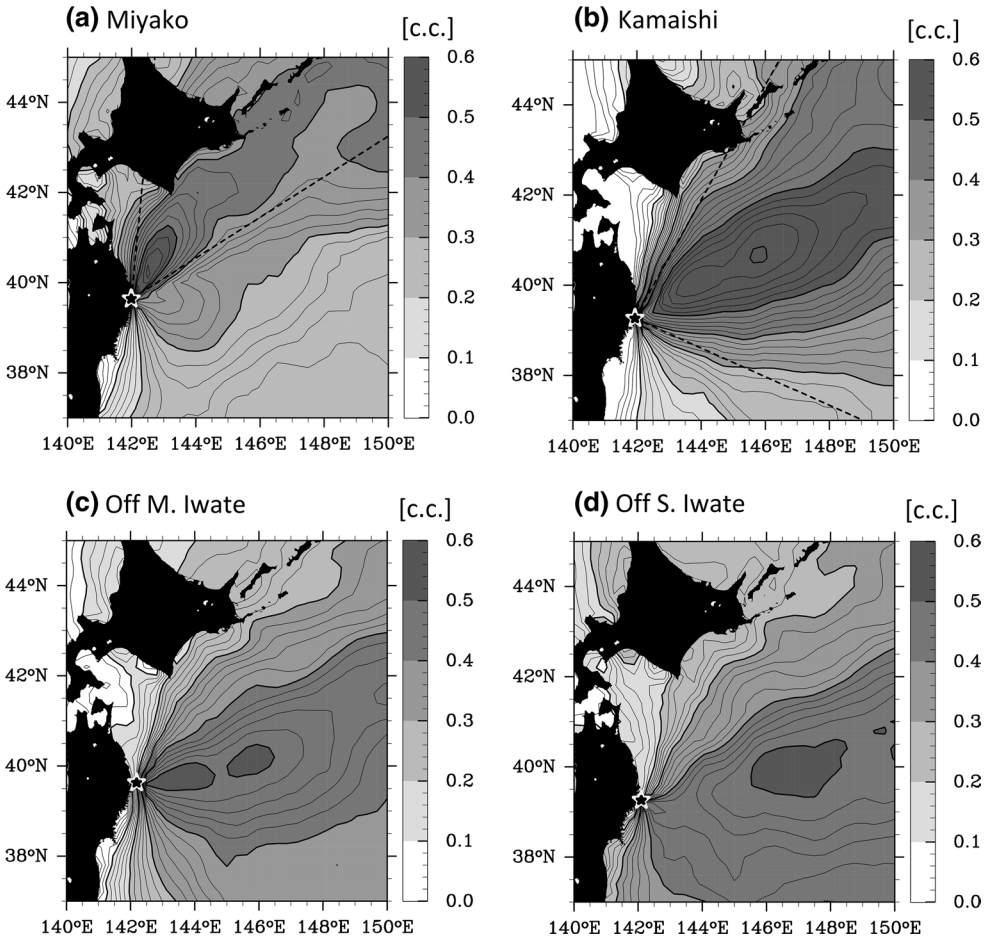

Fig. 12 Same as in Fig. 10a but for the NOWPHAS stations around Otsuchi Bay: Miyako Bay (**a**), Kamaishi Bay (**b**), M. Iwate (**c**), and S. Iwate (**d**)

refraction, diffraction, reflection, and shoaling to elucidate the cause of wave variation in the coastal region. However, waves at the monitoring point in Otsuchi Bay do not seem to be strongly influenced by the complicated shallow-water processes due to the following two reasons. First, Otsuchi Bay is characterized by the steep slope around the bay mouth (Fig. 1a), as is the case with the other ria bays on Sanriku coast, northeast of Japan. Second, the monitoring point is located at a depth of 40 m, which is not so shallow for the waves whose mean period is about 9 s to be affected strongly by the shallow water processes, according to Airy wave theory (e.g. Holthuijsen 2007). Therefore, the depth-induced refraction is unlikely to affect critically on the direction of waves which propagated toward the monitoring

point from the offshore region. Shoaling is also unlikely to alter significantly wave height at the monitoring point; actually, it has not been recognized at least visually yet. Moreover, the influence of reflection has not be detected clearly from the 2D wave spectra. These characteristics convince us of the robustness of the conclusion presented previously: waves generated by local southwestward wind in the northeastern offshore region that faces the bay mouth propagate directly as swells into the bay to affect predominantly the variation of waves in the bay.

However, the extent of contribution of swells to the wave variability in the bay might change depending on seasonal variation of the wind field in the offshore region, although the predominance of the swells must be robust through the year. In addition, influences of diffraction need to be considered around headlands of the bay. A numerical model that covers both shallow- and deep-water regions is required to estimate contribution of diffracted swells originated from the southeastern region as an example.

The ria bays are so various in form and size that it is empirically known that surface waves indicate significantly different characteristics from each other even in two adjacent bays (e.g. Kawaguchi et al. 2011). Figure 12 shows horizontal distributions of the maximum correlation coefficient between wind velocity and significant wave height observed at NOWPHAS stations around Otsuchi Bay: Miyako and Kamaishi stations are located inside of ria bays north and south of Otsuchi Bay, respectively, and the Off M. Iwate and Off S. Iwate stations are located in the open ocean east of Miyako and Kamaishi bays, respectively, as is shown in Fig. 1b. Interestingly, the horizontal distributions of the maximum correlation coefficient differ from one another among Otsuchi, Miyako, and Kamaishi bays, although the three bays are located within 42 km of each other (Figs. 11a, 12a, b). The distribution of the significant correlation (>0.4, $p < 0.05$) seems to depend on the direction extended from the mouth of each bay.

On the other hand, the horizontal distributions of the maximum correlation coefficient are comparatively analogous between the two offshore stations: M. Iwate and S. Iwate, although they are apart at almost the same distance between Miyako and Kamaishi bays. The difference between the coastal and offshore situations comes from the topographic effects, which are not so important for the offshore waves in deep ocean except for waves propagating eastward from the coast. It should be emphasized that the horizontal distribution of the offshore wind field which has dominant effects on coastal surface waves in a ria bay in Sanriku depends heavily on the topographic shape of the bay.

5 Summary

We began real-time monitoring of wind and surface waves in Otsuchi Bay, Iwate, Tohoku, Japan on October 3, 2012 using a mooring buoy with an ultrasonic anemometer and a single-mode GPS wave sensor. Horizontal wind velocity was recorded hourly for 600 h with 0.5-s intervals. Height, period, and direction of surface waves were estimated hourly from the 3D displacement of the buoy for 1200 h with 0.4-s intervals using the correction method developed by Harigae et al. (2004). Statistical data such as mean wind speed and direction, and significant wave height, period and direction, are distributed hourly in real time via the Internet along with a chart of their time series. The data can be viewed through cellular phones and used for fisheries and various operations in Otsuchi Bay.

In this study, we analyzed data monitored in the first 3 months in order to assess the variability and occurrence of wind and waves and to elucidate the main reasons for wave variation in Otsuchi Bay. The following results were obtained.

1. Surface waves in Otsuchi Bay were characterized by lower and longer waves in comparison with offshore waves as reported by previous studies (Sugimoto and Chikasawa 2008; Kawai et al. 2012).
2. The dominant waves in the bay propagated southwestward into the inner part of the bay from the bay mouth which opens to the ocean. The dominant wave direction was about 110° different from the mean wind direction in the bay.
3. The significant wave height in the bay was strongly correlated with that observed at the NOWPHAS site which is located offshore from the northeastern side of the bay, as is the case in other stations in the Pacific coast of Tohoku (Kawaguchi et al. 2011; Kawai et al. 2012).
4. Directional wave spectra in the bay revealed that swells propagated from the offshore region contribute 60–80 % of wave energy observed in the bay in the higher wave case, while wind waves generated in the bay contribute less than 15 % except for the lower wave case. These results support the conclusion that the variability of surface waves in Otsuchi Bay are strongly dependent on that of swells propagated from the northeastern offshore region into the bay.
5. The wave height in the bay was significantly correlated with the component of wind velocity toward Otsuchi Bay in the northeastern offshore region that faces the bay mouth. It indicates that waves generated by local southwesterly wind in the northeastern offshore region

propagate directly into the bay to affect predominantly the variation of waves in the bay.

These results expect the offshore wind field to provide information useful for predicting coastal waves in a ria bay in Sanriku such as Otsuchi Bay. However, it should be emphasized that the horizontal distribution of the offshore wind field, which has a significant effect on the surface waves in a ria bay, depends heavily on the topographic shape of the bay.

We have been continuing real-time monitoring of wind and surface waves in Otsuchi Bay. Seasonal and interanual variability of wind and waves is expected to be clarified in the future works.

Acknowledgments The authors would like to express their great appreciation to K. Kogure and A. Tsuda for their encouraging promotion of this study. We also are deeply appreciative of the Kamaishi-Tobu Fishermen's cooperative association (I. Ogawara, President) for providing facilities to moor the buoy in close vicinity to their aquaculture systems for the brown seaweed wakame. Mooring and maintenance of the buoy have been enormously supported by M. Kurosawa, M. Hirano, T. Suzuki, and other staff of the International Coastal Research Center, the Atmosphere and Ocean Research Institute at the University of Tokyo. We are also appreciative of the Shin-Otsuchi Fishermen's cooperative association and the Iwate Fisheries Technology Center for their helpful advice on operating the buoy. Wave data recorded by the NOWPHAS were downloaded from its website (http://www.mlit.go.jp/kowan/nowphas/), and sea–wind data simulated by the Japanese Meteorological Agency were from the data server of the GFD Dennou Club (http://database.rish.kyoto-u.ac.jp/arch/jmadata/data/gpv/netcdf/). Some of the figures were drawn using information from the GFD Dennou Library. Financial support for this study was provided by the Tohoku Ecosystem-Associated Marine Sciences, subsidized by the Ministry of Education, Culture, Sports, Science and Technology.

References

Agrawal YC, Terray EA, Donelan MA, Hwang PA, Williams AJ, Drennan W, Kahma K, Kitaigorodskii S (1992) Enhanced dissipation of kinetic energy beneath breaking waves. Nature 359:219–220

Ardhuin F, O'Reilly WC, Herbers THC, Jessen PF (2003) Swell transformation across the continental shelf. Part I: attenuation and directional broadening. J Phys Oceanogr 33:1921–1939. doi:10.1175/1520-0485(2003)033<1921:STATCS>2.0.CO;2

Booij N, Ris RC, Holthuijsen LH (1999) A third-generation wave model for coastal regions. 1. Model description and validation. J Geophys Res 104(C4):7649–7666. doi:10.1029/98JC02622

Buckley M, Lowe R, Hansen J (2014) Evaluation of nearshore wave models in steep reef environments. Ocean Dyn 64:847–862. doi:10.1007/s10236-014-0713-x

Craig PD, Banner ML (1994) Modeling wave-enhanced turbulence in the ocean surface layer. J Phys Oceanogr 24:2546–2559

Feddersen F, Trowbridge JH (2005) The effect of wave breaking on surf-zone turbulence and alongshore currents: a modeling study. J Phys Oceanogr 35:2187–2203

Forristall GZ (1978) On the statistical distribution of wave heights in a storm. J Geophys Res 83(C5):2353–2358. doi:10.1029/JC083iC05p02353

Harigae M, Yamaguchi I, Kasai T, Igawa H, Nakanishi H, Murayama T, Iwanaka Y, Suko H (2004) Abreast of the waves: open-sea sensor to measure height and direction. GPS World 16:16–27

Hofmann-Wellenhof B, Lichtenegger H, Walse E (2007) GNSS-global navigation satellite systems, GPS, GLONASS, Galileo, and more. Springer, New York, p 548

Holthuijsen LH (2007) Wave in oceanic and coastal waters. Cambridge University Press, Cambridge, p 387

Isobe M, Kondo K, Horikawa K (1984a) Extension of MLM for estimating directional wave spectrum. Proc. Symp. on Description and Modeling of Directional Seas A-6, p 15

Isobe M, Kondo K, Horikawa K (1984b) Extension of MLM for estimating directional wave spectrum. Proc Coast Eng Jpn Soc Civ Eng 31:173–177 **(in Japanese)**

Kawaguchi K, Kawai H, Satoh M, Chimoto T, Yamaya S (2011) Correlativity of observed wave data between GPS-mounted buoy and coastal wave gauge on the northern Pacific side in Tohoku district. J Jpn Soc Civ Eng Ser B2 67(2):I_436–I_440 **(in Japanese with English abstract)**

Kawai H, Satoh M, Kawaguchi K, Seki K (2012) Offshore wave characteristics observed by GPS buoys on the Tohoku to Shikoku district coast of the Pacific ocean, Japan. Tech Note Port Airpt Res Inst 1249:1–51 **(in Japanese with English abstract)**

Kawamata S (2001) Effect of waves on grazing by sea urchins and abalone on the coast of northern Japan. Bull Fish Res Agency 1:59–107 **(Doctor thesis in Japanese with English abstract and captions)**

Komatsu K, Masuda A (1996) A new scheme of nonlinear energy transfer among wind waves: RIAM method-algorithm and performance. J Oceanogr 52:509–537

Large W, Pond S (1981) Open ocean momentum flux measurements in moderate to strong winds. J Phys Oceanogr 11:324–336

Mei CC (1989) The applied dynamics of ocean surface waves, 2nd edn. World Scientific, Singapore, p 760

Melville WK (1996) The role of surface wave breaking in air–sea interaction. Annu Rev Fluid Mech 28:279–321

Otobe H, Onishi H, Inada M, Michida Y, Terazaki M (2009) Estimation of water circulation in Otsuchi Bay, Japan inferred from ADCP observation. Coast Mar Sci 33(1):78–86

Portilla J, Ocampo-Torres FJ, Monbaliu J (2009) Spectral partitioning and identification of wind sea and swell. J Atmos Ocean Technol 26:107–122. doi:10.1175/2008JTECHO609.1

Ris RC, Holthuijsen LH, Booij N (1999) A third-generation wave model for coastal regions. 2. Verification. J Geophys Res 104(C4):7667–7681. doi:10.1029/1998JC900123

Sugimoto S, Chikasawa M (2008) A study on Japanese coastal wave characteristics using coastal wave observation by Japan Meteorological Agency. Weather Serv Bull 75:S77–S95 **(in Japanese)**

The WAMDI Group (1988) The WAM Model-A third generation ocean wave prediction model. J Phys Oceanogr 18:1775–1810. doi:10.1175/1520-0485(1988)018<1775:TWMTGO>2.0.CO;2

Tolman HL (2002) User manual and system documentation of WAVEWATCH-III version 2.22. NOAA/NWS/NCEP/OMB technical note, 222, p 133

Waseda T, Sinchi M, Kiyomatsu K, Nishida T, Takahashi S, Asaumi S, Kawai Y, Tamura H, Miyazawa Y (2014) Deep water observations of extreme waves with moored and free GPS buoys. Ocean Dyn 64:1269–1280. doi:10.1007/s10236-014-0751-4

Zijlema M, Stelling G, Smit P (2011) SWASH: an operational public domain code for simulating wave fields and rapidly varied flows in coastal waters. Coast Eng 58:992–1012. doi:10.1016/j.coastaleng.2011.05.015